

UNCLASSIFIED

Defense Technical Information Center
Compilation Part Notice

ADP013126

TITLE: Room Temperature Single Electron Devices by STM/AFM
Nano-Oxidation Process

DISTRIBUTION: Approved for public release, distribution unlimited
Availability: Hard copy only.

This paper is part of the following report:

TITLE: Nanostructures: Physics and Technology International Symposium
[8th] Held in St. Petersburg, Russia on June 19-23, 2000 Proceedings

To order the complete compilation report, use: ADA407315

The component part is provided here to allow users access to individually authored sections of proceedings, annals, symposia, etc. However, the component should be considered within the context of the overall compilation report and not as a stand-alone technical report.

The following component part numbers comprise the compilation report:

ADP013002 thru ADP013146

UNCLASSIFIED

Room temperature single electron devices by STM/AFM nano-oxidation process

Kazuhiko Matsumoto

Electrotechnical Laboratory, MITI, 1-1-4, Umezono, Tsukuba, 305-8568, Japan
e-mail:kmatumot@etl.go.jp

Abstract. A single electron transistor (SET) and a single electron memory were fabricated using the improved pulse-mode AFM nano-oxidation process. A single electron transistor which works as an electrometer for detecting the potential of the memory node of the single electron memory showed the clear Coulomb oscillation characteristics with the periods of 2.1 V at room temperature. A single electron memory showed the hysteresis loop by the return trip of the memory bias when starting from 0 V to 10 V and again coming back to 0 V.

Introduction

A various types of single electron transistors and memories were, so far, studied. Almost all single electron devices so far studied adopted the self-organized nano-structure because of the difficulty of the artificial fabrication process of the nano-structure. The some examples of the self-organized nano-structure for the single electron devices are the polycrystalline silicon film [1], the poly-crystal silicon dot [2], and the squeezed delta-doped GaAlAs/GaAs layer [3] for the multi-tunnel junctions and/or memory node. They showed the clear single electron device characteristics such as the digitized threshold voltage shifts [1] or hysteresis loop [3] by the injected few number of electrons. Those devices, however, include the problem of the poor reproducibility of the device characteristics because of the application of the spontaneously formed nano-structures. On the other hand, in the present paper, we show the new device fabrication process [4–6], which could artificially fabricate the few tens of nano-meter order small structure and room temperature operated single electron transistor and single electron memory were realized.

1. AFM nano-oxidation process

The new fabrication process used the atomic force microscopy (AFM) cantilever as an ultra small cathode, and pulse bias was applied between cantilever and the 2.5 nm thick titanium (Ti) thin film that was on the atomically flat α -Al₂O₃ substrate as shown in Fig. 1. AFM nano-oxidation process so far we proposed used DC bias between the cantilever and the titanium metal, and the surface of the Ti metal was anodized to form the oxidized titanium line (TiO_x) which works as a tunnel junction for the single electron devices [4–6]. During this DC-mode AFM nano-oxidation process, however, the positive hydrogen ions H⁺ formed the space charge at the front end of the TiO_x/Ti interface, which prevents the further oxidation. This causes the difficulty for the deeper oxidation. In order to solve the problem, the $\pm 1.5 \sim 2$ V pulse bias was applied instead of the DC bias between the conductive AFM cantilever and the Ti metal [7]. The negative pulse anodized the surface of the metal and the positive pulse neutralized the positive space charge from the front end of TiO_x. Therefore, using the pulse bias for the oxidation, the deeper oxidation becomes possible than the DC bias at the same applied bias. In another words, a narrower and deeper

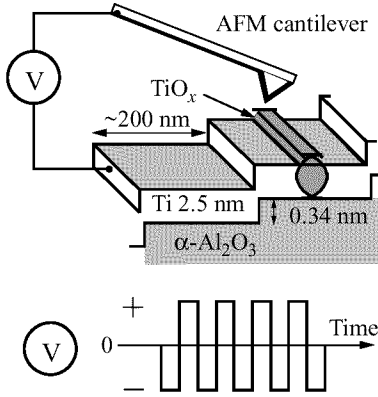


Fig. 1. Schematic diagram of pulse-mode AFM nano-oxidation process on atomically flat $\alpha - \text{Al}_2\text{O}_3$ substrate.

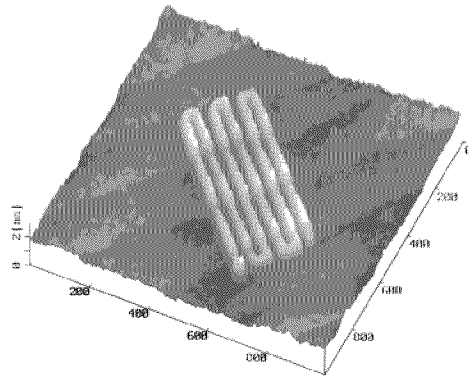


Fig. 2. AFM image of TiO_x line folded six times on atomically flat $\text{Ti}/\alpha - \text{Al}_2\text{O}_3$ substrate made by pulse-mode AFM nano-oxidation process. Linewidth is 20 nm, and line height 1.2 nm.

oxidized Ti line could be formed using the lower applied pulse bias. Figure 2 shows the AFM image of the TiO_x line folded six times on the atomically flat $\text{Ti}/\alpha - \text{Al}_2\text{O}_3$ substrate fabricated by the present new AFM nano-oxidation process. The line width is 20 nm, and line height 1.2 nm. The smooth and uniform TiO_x line was obtained reproducibly. Using this new process, the single electron transistor and the single electron memory were fabricated.

2. Single electron transistor

Figure 3 shows the schematic structure and AFM image of the fabricated one island side gate single electron transistor (SET) on the atomically flat $\alpha - \text{Al}_2\text{O}_3$ substrate. Using the pulse mode AFM nano-oxidation process, two tunnel junctions for SET were formed by TiO_x lines. The size of the tunnel junction is 19 nm (width) \times 26 nm (length) \times 2 nm (thickness) and the island size is 8 nm \times 26 nm.

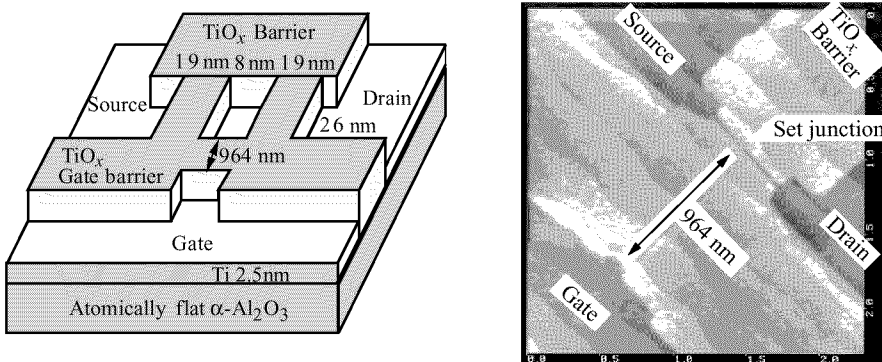


Fig. 3. Schematic structure and plain AFM image of the fabricated one island side gate SET on the atomically flat substrate. Two tunnel junction size is 19 nm (width) \times 26 nm (length) \times 2 nm (thickness) and island size 8 nm \times 26 nm.

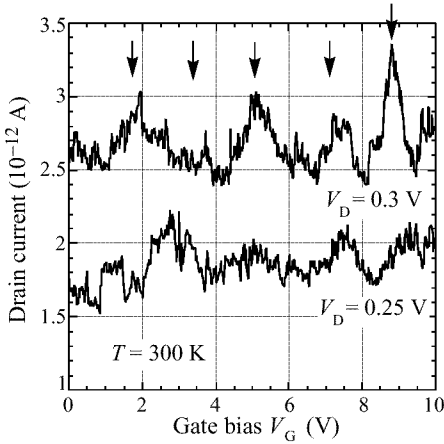


Fig. 4. Dependence of Coulomb oscillation on drain bias at room temperature. $V_D = 0.25$ V and 0.3 V.

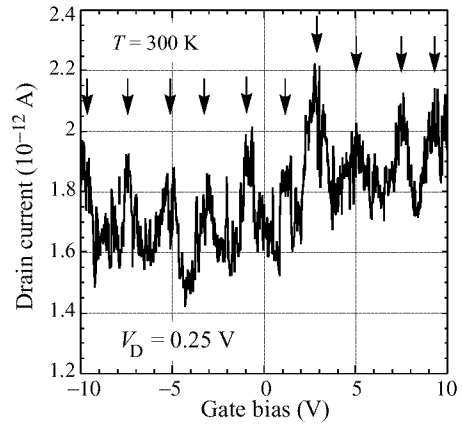


Fig. 5. Symmetrical characteristics of Coulomb oscillation against gate bias at room temperature.

The width of the gate insulator for the side gate SET was increased up to 964 nm to completely prevent the gate leakage current at room temperature. (In the previous work, the width of the gate insulator was 300 nm).

Figure 4 shows the drain current-gate bias characteristics of the SET at room temperature using the drain bias as a parameter. The drain current of the SET oscillates with the period of 2.1 V at room temperature in the gate bias range of 0 V to 10 V at the drain bias of $V_D = 0.25$ V and 0.3 V. Five peaks are clearly seen for the each drain bias condition. The current modulation rate is from 20% to 30%. Even at the different drain bias, the drain current shows the oscillation peaks at the same gate bias points. The gate capacitance estimated from the periods of the Coulomb oscillation is 8×10^{-20} F.

Figure 5 shows the drain current-gate bias characteristics when the gate bias was changed from -10 V to 10 V at the drain bias of $V_D = 0.25$ V. The peaks of the Coulomb oscillation appear periodically and symmetrically against the plus and minus region in the gate bias. Thus, the fabricated SET shows the clear gate action even at room temperature.

3. Single electron memory

Figure 6 shows the equivalent circuit of the single electron memory which consists of the multi-tunnel junction and the normal memory capacitance. The memory node of the single electron memory where small number of electrons are stored is connected by the single electron transistor (SET) through the normal capacitance C_g . Using the equivalent circuit of the single electron memory shown in Fig. 6, the principle of the operation of the single electron memory is explained as follows. By increasing the memory bias, V_{MEM} , the potential of the memory node V_t also increases in proportion to the ratio of the memory capacitance C_{gt} and the multi-tunnel junction capacitance C_{tt} , i.e.,

$$V_t = V_{MEM} C_{gt} / (C_{tt} + C_{gt}). \quad (1)$$

When the potential of the memory node V_t becomes larger than the Coulomb gap bias of the multi-tunnel junction V_0 , one electron can pass through the multi-tunnel junction to reach the memory node, which lowers the potential of the memory node as $e / (C_{tt} + C_{gt})$,

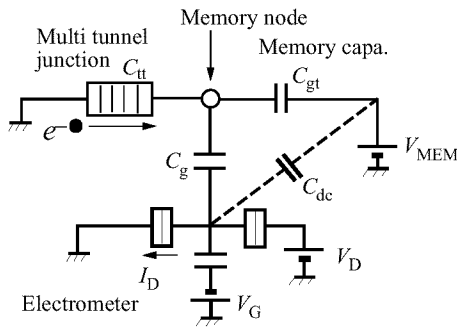


Fig. 6. Equivalent circuit of single electron memory.

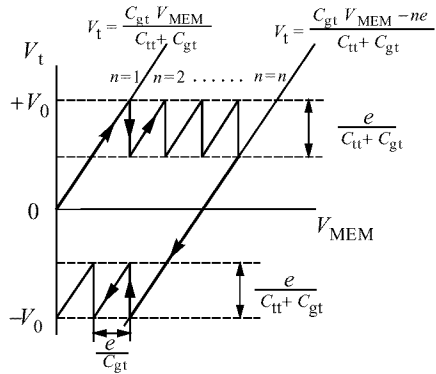


Fig. 7. Dependence of memory node potential, V_t , on memory bias, V_{MEM} .

and the second electron can not pass through the multi-tunnel junction. By increasing the memory bias further, the potential of the memory node V_t again reaches to the Coulomb gap bias, V_0 , then the second electron can pass through the multi-tunnel junction to reach the memory node. Thus the one by one electron transfer becomes possible through the multi-tunnel junction to the memory node. When the n electrons are stored at the memory node, the potential of the memory node which is lowered by n electrons is described as follows:

$$V_t = (V_{MEM}C_{gt} - ne)/(C_{tt} + C_{gt}), \tag{2}$$

where e is the electron charge. When the memory bias, V_{MEM} comes back to the lower bias, the potential of the memory node V_t goes into the negative region because of the stored n electrons. When V_t becomes smaller than the negative Coulomb gap bias of the multi-tunnel junction $-V_0$, the electrons are ejected one by one to the ground. Therefore, the potential of the memory node V_t shows the hysteresis loop. The relation between the memory node potential V_t and the memory bias V_{MEM} is shown in Fig. 7. Thus, few number of electrons are memorized at the memory node for few hundred seconds and this device works as a single electron memory. The change of the potential at the memory node by the injection and the ejection of electrons through the multi-tunnel junction is detected by the change of the drain current of the SET, which works as an electrometer. The change of the drain current of the electrometer is considered to be linearly proportional to the potential change of the memory node.

Figure 8 shows the schematic structure of the fabricated single electron memory which sits on the atomically flat $\alpha - Al_2O_3$ substrate. Figure 9 is the AFM image of the multi-tunnel junction area and two tunnel SET junctions of the fabricated single electron memory. The device consists of the multi-tunnel junction and normal capacitance for the memory and two tunnel junctions for the single electron transistor. There are four electrodes, i.e. the memory bias electrode for the memory, the source, drain and gate electrodes for the single electron transistor. The multi tunnel junction consists of five or seven tunnel junctions which are 15 ~ 25 nm in width, 15 ~ 25 nm in length, 2 nm in thickness, and the spacing between them is 10 ~ 15 nm. The normal memory capacitance is 341 nm in width and 15 ~ 25 nm in length, and 2 nm in thickness. The area between the multi-tunnel junction and the memory capacitance is designated as a memory node where few number of electrons are stored. The distance between the memory node and the island of the single electron transistor is 486 nm which determined the sensitivity of the SET. The size of the two tunnel

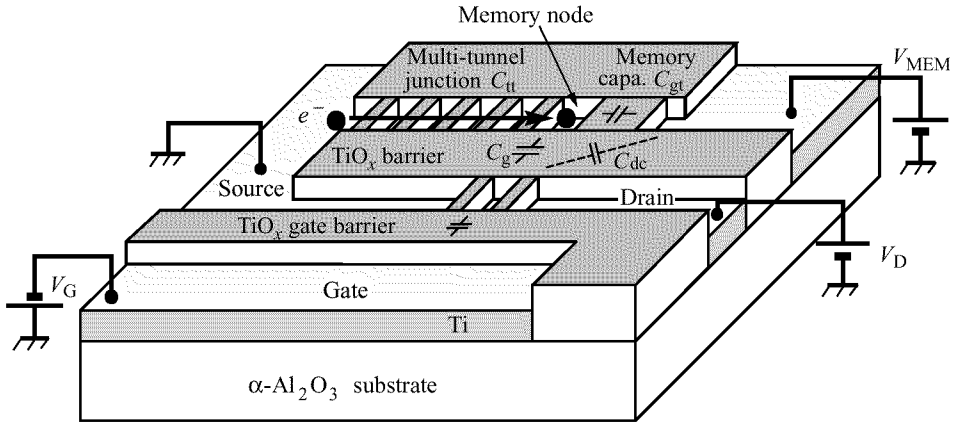


Fig. 8. Schematic structure of single electron memory on atomically flat $\alpha - \text{Al}_2\text{O}_3$ substrate made by pulse-mode AFM nano-oxidation process.

junctions for SET is 15 ~ 25 nm in width, 15 ~ 25 nm in length, 2 nm in thickness, and the spacing between them is 10 ~ 15 nm, i.e., the island size is 10 ~ 15 nm \times 15 ~ 25 nm.

For the measurement of the single electron memory, the condition of the electrometer was set as the drain bias of $V_D = 3$ V, and the gate bias of $V_G = 1.5$ V to detect the potential change of the memory node. Figure 10 shows the drain current of the electrometer, i.e., the single electron transistor versus the memory bias characteristics at room temperature. When the memory bias V_{MEM} of the single electron memory increases from 0 V to 10 V, the drain current of the electrometer increases at the beginning and begins to oscillate. The drain current oscillation is attributed to the two effects, i.e., one is owing to the injection of the individual electrons through the multi-tunnel junction to the memory node which lowers the potential of the memory node, and the other is owing to the direct coupling of the memory bias to the island of the single electron transistor which causes the Coulomb oscillation. When the memory bias comes back from 10 V to 0 V, the drain current follows the different trace owing to the stored electrons at the memory node and shows the clear hysteresis loop even at room temperature. The measured hysteresis loop is quite similar to that shown in Fig. 2(b). Owing to the large noise level in Fig. 10, however, it is difficult to distinguish the oscillation peaks owing to the electron injection to the memory node from noise peaks.

The time transient of the drain current at room temperature when the memory bias was suddenly cut off from 10 V to 0 V showed the step-like transient trace indicating the one by one electron ejection from the memory node to the ground. The retention time is found to be 600 seconds.

The number of electrons stored in the memory node when the memory bias of 10 V was applied could be calculated from Eq. (2) and

$$n = (C_{gt} V_{MEM} - (C_{tt} + C_{gt}) V_t) / e, \quad (3)$$

where $V_{MEM} \gg V_t$ when $V_{MEM} = 10$ V. Therefore, n is roughly calculated as

$$n = C_{gt} V_{MEM} / e. \quad (4)$$

Using the three dimensional simulator, the three dimensional Poisson's equation was solved for the single electron memory structure and the memory capacitance is calculated to be as

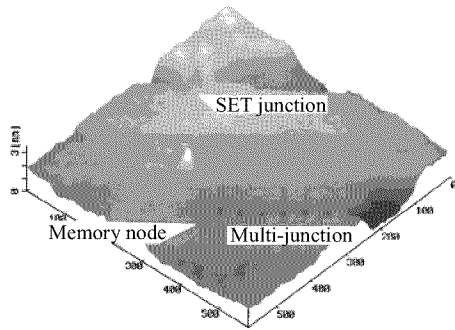


Fig. 9. Plain AFM image of the fabricated single electron memory on atomically flat substrate. Multi-tunnel junctions for memory and SET junctions for electrometer are seen.

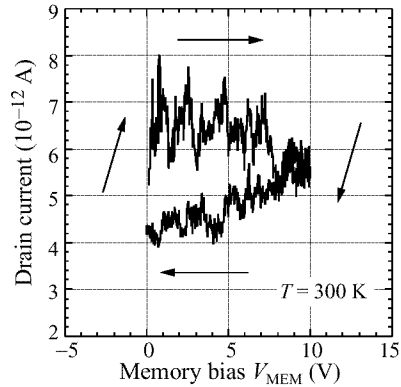


Fig. 10. Hysteresis loop of single electron memory at room temperature. Gate bias and drain bias for SET were set at $V_G = 1.5$ V and $V_D = 3$ V, respectively. Memory bias was applied from $V_{MEM} = 0$ V to 10 V and back to 0 V.

$C_{gt} = 4 \times 10^{-19}$ F. Using this value, the number of electrons stored in the memory node is calculated to be about $n = 25$.

Using the improved pulse-mode AFM nano-oxidation process, the single electron memory was fabricated on the atomically flat $\alpha - \text{Al}_2\text{O}_3$ substrate. The single electron memory stored about 25 electrons at the memory node with the applied memory bias of 10 V, and showed the hysteresis loop even at room temperature. The retention time of the single electron memory is 600 seconds.

4. Conclusions

Using the improved pulse-mode AFM nano-oxidation process, the single electron transistor and single electron memory were fabricated on the atomically flat $\alpha - \text{Al}_2\text{O}_3$ substrate. The single electron transistor shows the Coulomb oscillation with the periods of 2.1 V at room temperature. The single electron memory shows the hysteresis loop even at room temperature.

References

- [1] K. Yano, T. Ishii, T. Hashimoto, T. Kobayashi, F. Murai and K. Seki, *Technical Digest of International Electron Device Meeting*, 541 (1993).
- [2] S. Tiwari, F. Rana, K. Chan, H. Hanafi, W. Chan and D. Buchanan, *Technical Digest of International Electron Device Meeting*, 521 (1995).
- [3] K. Nakazato, T. J. Thornton, J. White and H. Ahmed, *Electron. Lett.* **29**, 384 (1993).
- [4] K. Matsumoto, S. Takahashi, M. Ishii, M. Hoshi, A. Kurokawa, S. Ichimura and A. Ando, *Jpn. J. Appl. Phys.* **34**, 1387 (1995).
- [5] K. Matsumoto, M. Ishii, K. Segawa, Y. Oka, B. J. Vartanian and J. S. Harris, *Appl. Phys. Lett.* **68**, 34 (1996).
- [6] K. Matsumoto, *Proceedings of IEEE* **85**, 612 (1997).
- [7] J. A. Dagata, T. Inoue, J. Itoh, K. Matsumoto and H. Yokoyama, *J. Appl. Phys.* **84**, 6891 (1998).